Bull. Mater. Sci., Vol. 31, No. 3, June 2008, pp. 507–510. © Indian Academy of Sciences.

Nanocrystalline spinel ferrites by solid state reaction route

T K KUNDU* and S MISHRA

Department of Physics, Visva-Bharati, Santiniketan 731 235, India

Abstract. **Nanostructured $NiFe_2O_4$, $MnFe_2O_4$ and $(NiZn)Fe_2O_4$ were synthesized by aliovalent ion doping using conventional solid-state reaction route. With the doping of Nb_2O_5, the size of $NiFe_2O_4$ is reduced down to 33 nm. Similarly, nanostructured manganese ferrites ($MnFe_2O_4$) with diameters in the range of 45–30 nm were synthesized by Ti^{4+} ion doping. Particle diameters in all the specimens are found to decrease with increasing dopant content. The substitution of Nb^{5+} or Ti^{3+} ions essentially breaks up the ferrimagnetically active oxygen polyhedra. This created nanoscale regions of ferrites. Saturation magnetization and coercive field show a strong dependence on the size of the ferrite grains. Superparamagnetic behaviour is observed from the Mössbauer spectra of nanostructured $NiFe_2O_4$, if the particle size is reduced to 30 nm. Zero field cooled and field cooled curves from 30 nm sized $MnFe_2O_4$ particles showed a peak at T_B (~ 125 K), typical of superparamagnetic blocking temperature. These results are explained in terms of core/shell structure of the materials. The d.c. resistivity of the doped specimens decreases by atleast five orders of magnitude compared to pure sample. This is ascribed to the presence of an interfacial amorphous phase between the sites.**

Keywords. **Nanoparticles; nanoferrites; electrical conductivity.**

1. Introduction

During the last few years nanoscale spinel ferrites have drawn a major attention because of their technological importance in magnetic recording, magnetic fluids and catalyst. Nanoferrites are usually prepared using various physical and chemical methods like ball milling, microwave plasma, coprecipitation (Ferele and Baberschke 1987; Tang *et al* 1991; Chatterjee *et al* 1993). The synthesis of ferrite nanoparticles is of great interest for studying and tailoring of specific magnetic properties. It was found that the doping of lanthanum impurity ions could suppress the long-range ferroelectric order in the lead zirconium titanate (PZT) system (Li *et al* 1995; Xu *et al* 1995). The nanostructured phase was found to be induced with increasing La impurity content in the ferroelectric ceramic system. A similar approach is made in the present case and a set of nanocrystalline spinel ferrites are prepared using the conventional ceramic route with suitable doping by aliovalent ions (Kundu and Chakravorty 1999). Nanostructured $NiFe_2O_4$, $MnFe_2O_4$ and $(NiZn)Fe_2O_4$ were synthesized by using Nb^{5+} or Ti^{3+} ion doping. The experimental results are reported in this paper.

2. Nanostructured $NiFe_2O_4$

The samples were prepared with the starting materials, $Ni(NO_3)_2$, Fe_2O_3 and Nb_2O_5. The composition of the materials is represented by zNb_2O_5, $(0{\cdot}5 - z)$ NiO, $0{\cdot}5Fe_2O_3$ with z having values 0·0, 0·10 and 0·20, respectively. Weighed amounts of staring materials were taken in a mortar and mixed for a duration of 2–3 h under acetone. The powders were calcined in air for 2 h at 800°C. The calcined powders were pressed into pellet and sintered at 1000°C for 2 h.

The crystalline phases precipitated in the sintered specimens were investigated using X-ray diffractograms. The patterns of the samples show that all the expected lines of the $NiFe_2O_4$ spinel structure are present and few lines of Nb_2O_5 only appears in specimen 'c' which is doped with $x = 0{\cdot}20$. Thus the present set of spinel ferrites are formed with Nb^{5+} getting into the structure.

The grain size of the crystallites in the sintered specimens was estimated from the broadening of the most intense X-ray line for $NiFe_2O_4$ by using Scherrer formula. With the doping of Nb_2O_5, the size of the $NiFe_2O_4$ grain is reduced. The lowest size of $NiFe_2O_4$ grain is 30 nm. Figure 1 is a typical transmission electron micrograph for the specimen c of doped $NiFe_2O_4$. The average values of the particle size are calculated from the micrographs. The results are given in table 1. It is seen that the grain size of the crystallites in undoped $NiFe_2O_4$ specimen is 2 μm. The grain sizes in specimen b doped with 10 mole% and specimen c doped with 20 mole% are 67 nm and 30 nm, respectively. Nb^{5+} ions go into the structure of the doped specimens as it is evident from the broadening of the diffraction lines. Since the ionic radius of Nb^{5+} (0·07 nm) is quite close to that of Ni^{2+}, Nb^{5+} will substitute the Ni^{2+} sites with the creation of vacancy. The presence of Nb^{5+} ions and the resultant vacancies can break the coupling of

*Author for correspondence (tkkundu1968@yahoo.com)

ferrimagnetically active oxygen polyhedra and the growth can be inhibited as it occurred in ferroelectric system by suppressing the long range ferroelectric ordering (Li *et al* 1995; Xu *et al* 1995).

Magnetization versus field for the sintered samples was measured using a PAR Vibrating Sample Magnetometer. The values of the room temperature saturation magnetization (M_s) and coercive field (H_c) as a function of particle diameter are given in table 1. M_s were measured at a magnetic field of 2000 Oe. It is seen that the substitution of Nb^{5+} ion decreases the magnetization and increases the coercive field as the particle size of $NiFe_2O_4$ is reduced. M_s decreases from 42 emu/g to 15 emu/g as the particle diameter of $NiFe_2O_4$ is decreased from 1 μm to 30 nm (Mishra *et al* 2006). This behaviour can be explained introducing core-shell model of magnetic nanoparticles (Sato *et al* 1987; Kundu and Chakravorty 1999). In the present case, as the Ni^{2+} ions in $NiFe_2O_4$ grains are substituted by Nb^{5+} ions, a layer of Nb^{5+} doped $NiFe_2O_4$ phase is generated surrounding the undoped $NiFe_2O_4$ region. The doped region of particles is defined as shell and the undoped regions as core. The shell has a smaller magnetization compared to the core due to the closed shell structure of Nb^{5+}. The shell is visualized to be the zone in which Nb^{5+} ions have created vacancies and the superexchange interaction has been destroyed. Earlier core-shell morphology in nickel ferrite nanoparticles consisting of a ferrimagnetically aligned core spins and a spin-glass like surface layer was introduced to explain the reduction and non-attainment of saturation magnetization (Nathani *et al* 2005). In those cases the spin–glass like surface originated due to broken exchange bonds at the surface of the nanoparticles. H_c increases from 68 to 111 Oe as the particle diameter is decreased. According to the conventional theory for ferromagnetic particles, the coercivity, H_c, can be written as (Kundu and Chakravorty 1999)

$$H_c = (2K/M_s)[1 - (T/T_B)^{0.5}], \quad (1)$$

where M_s is the saturation magnetization, K the volume magnetocrystalline anisotropy, T_B the blocking temperature, which is proportional to the value of the magnetic anisotropy energy KV, where V is the volume of the ferromagnetic particle. Previous reports show that T_B decreases when the particle size is decreased. The decrease in T_B may cause a reduction of H_c according to (1). Similarly a decrease in M_s due to lowering of particle size may also result in an increase in H_c according to (1). Here, the experimental results show that H_c for all the specimens increases with the decrease of particle diameter. It means the saturation magnetization is playing a dominant role in determining the variation of coercive field with particle size. A lowering of the value of M_s with particle size can thus explain the increase of H_c with a decrease in particle size of $NiFe_2O_4$. The Mössbauer spectrum from specimen '*a*' consists of six-finger pattern. However, the spectra from the doped specimens contain a doublet in addition to the six-finger pattern (figure 2). The doublet may arise due to the smaller particles in the specimens and is known as superparamagnetic doublet. Larger sized particles are also present in the doped specimens and therefore, the superparamagnetic doublet appears in the background of six-finger pattern.

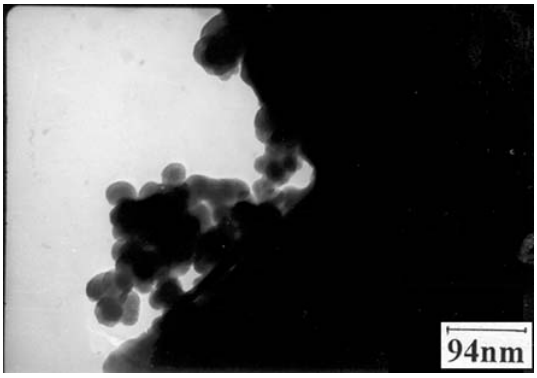

Figure 1. Transmission electron micrograph of 20 mole% Nb_2O_5 doped $NiFe_2O_4$.

3. Nanostructured $MnFe_2O_4$

The target compositions of the materials are given in table 2. Weighed amounts of mixed precursor are calcined at 800°C for 2 h in air. The powders are taken in a mold for cold compaction at a pressure of 5 bars and finally sintered in air for 2 h at 1100°C.

X-ray diffraction patterns of the sintered samples show that all the expected lines of the $MnFe_2O_4$ spinel structure are present (Mishra *et al* 2006). Thus the present set of spinel ferrites are formed with Ti^{4+} getting into the structure. The grain diameters were calculated from X-ray line broadening. The grain size of undoped sample remains in the order of a few micrometer. With the doping of TiO_2, the size of $MnFe_2O_4$ grains is gradually reduced down to 30 nm. Figure 3 shows a typical TEM picture for the specimen doped with 20 mole% of dopant. The room temperature saturation magnetization and coercivity for the samples are given in table 2. This magnetic behaviour is quite similar in nature to that obtained for the nanostructured $NiFe_2O_4$ and thus a similar explanation is also valid for $MnFe_2O_4$. In this case some of the Mn^{2+} ions in $MnFe_2O_4$ specimens are substituted by Ti^{4+} ions during processing. Thus the vacancies should be in Mn^{2+} sites. The resultant vacancies in the presence of Ti^{4+} ions are believed to break the coupling of ferrimagnetically active oxygen polyhedra.

The resistivity decreases significantly as the $MnFe_2O_4$ samples are doped with TiO_2. Previous reports show that the electrical resistivity of iron-based samples arises due to a small polaron hopping between Fe^{2+} and Fe^{3+} sites (Bramha *et al* 1991). We have fitted the data to Mott's

Table 1. Particle diameter, saturation magnetization and coercive field for the $NiFe_2O_4$ samples.

Specimen no.	Sample composition (mole%)	Particle diameter from TEM	H_c (Oe)	M_s (emu/g)
a	$50NiO$, $50Fe_2O_3$	~2 μm	67·98	42·23
b	$10Nb_2O_5$, $40NiO$, $50Fe_2O_3$	67 nm	90·00	29·02
c	$20Nb_2O_5$, $30NiO$, $50Fe_2O_3$	30 nm	111·00	14·96

Table 2. Particle diameter, saturation magnetization and coercive field for the $MnFe_2O_4$ samples.

Specimen no.	Sample composition (mole%)	Particle diameter from TEM	Coercive field (Oe)	M_s (emu/g)	ε_p
1	$50MnO$, $50Fe_2O_3$	0·5 μm	44	37·0	1·2
2	$10TiO_2$, $40MnO$, $50Fe_2O_3$	45 nm	79	1·6	1·5
3	$20TiO_2$, $30MnO$, $50Fe_2O_3$	30 nm	2929	0·45	1·7

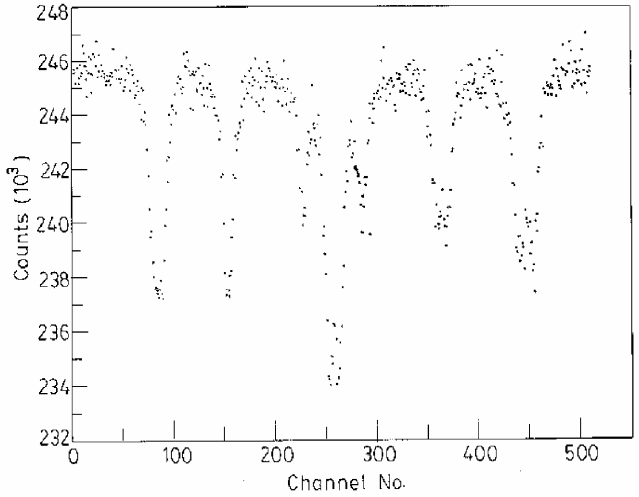

Figure 2. Mössbauer spectrum of 20 mole% Nb_2O_5 doped $NiFe_2O_4$.

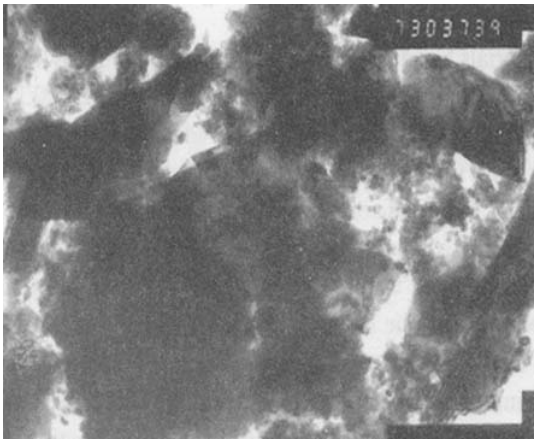

Figure 3. Transmission electron micrograph of the 20 mole% TiO_2 doped $MnFe_2O_4$.

equation for small polaron hopping between localized states. The equation describing such a transport is given by (Mott 1969)

$$\rho = [kTR/(\nu_0 e^2 C(1-C))]\exp(2\alpha R)\exp(W/kT), \quad (2)$$

where R is the average hopping distance, ν_0 the optical phonon frequency, C the ratio of Fe^{2+} ion concentration to the total Fe ion concentration, α^{-1} the localization length describing the localized states at each transition metal ion site and W the activation energy for the hopping conduction. The parameters W, α, R, C and ν_0 have reasonable values, and show strong localization. As the value of C in all the specimens is close to unity, the major fraction of transition metal ions in the specimens remains as Fe^{2+}. Effective dielectric constants (ε_p) of the interfacial amorphous phase have been estimated from W and R using the following relation (Bogomolov *et al* 1968)

$$\varepsilon_p = (e^2/2WR)(6/\pi)^{1/3}. \quad (3)$$

The values of effective dielectric constant are given in the last column of table 2. The small values of dielectric constants confirm the presence of an interfacial phase that controls the d.c. electrical properties of the specimens.

4. Nanostructured $(NiZn)Fe_2O_4$

Nanostructured $(NiZn)Fe_2O_4$ materials were generated using similar approach as that of $NiFe_2O_4$ and $MnFe_2O_4$. The target compositions were zNb_2O_5, $(0{\cdot}5-z)/2MnO$, $(0{\cdot}5-z)/2ZnO$, $0{\cdot}5Fe_2O_3$ with $z = 0{\cdot}0$, $0{\cdot}10$, $0{\cdot}20$ and $0{\cdot}25$, respectively. Final products of nanostructured $(NiZn)Fe_2O_4$ magnetic materials in the form of pellet were developed by using the same experimental procedure as discussed in §2. Figure 4 shows a typical TEM picture for the 20 mole% doped $(NiZn)Fe_2O_4$. The lowest diameter of 48 nm is generated with 25 mole% Nb_2O_5 doping. It is observed that the size of $(NiZn)Fe_2O_4$ grain gradually

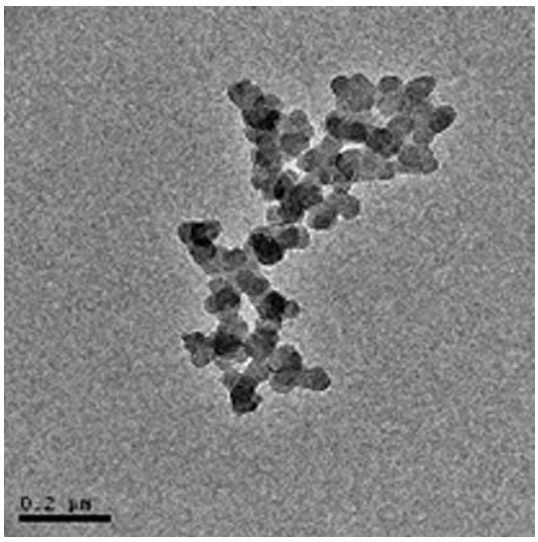

Figure 4. Transmission electron micrograph of the 20 mole% TiO_2 doped $NiZnFe_2O_4$.

decreases from 1 μm to 48 nm with the increase of Nb^{5+} content. Magnetic measurement shows that M_s decreases from 20 emu/g to 4 emu/g and H_c increases with the decrease of $(NiZn)Fe_2O_4$ diameter. The microstructural and magnetic results are very similar to that of nanostructured $NiFe_2O_4$ and $MnFe_2O_4$ prepared through the same method. Therefore, these experimental results support well the arguments given in §§2 and 3 about the formation of nanostructured materials by aliovalent ion doping.

5. Summary

In summary, we have explored the solid-state reaction route for the production of nanocrystalline spinel ferrites. A series of spinel ferrites like $NiFe_2O_4$, $MnFe_2O_4$ and $(NiZn)Fe_2O_4$ are developed by doping with Nb^{5+}/Ti^{3+} ions using this conventional ceramic processing route. Nanostructured ferrite particles are found to evolve with increasing concentration of dopant ions. Since the ionic radius of the dopant is quite close to that of Ni^{2+}or Mn^{2+} or Zn^{2+} ions, it substitutes the ions with the creation of vacancy. The presence of dopant ions and the resultant vacancies are believed to break the coupling of ferrimagnetically active oxygen polyhedra. Saturation magnetization and coercive field show a strong dependence on the size of the ferrite grains. The Mössbauer spectrum of nanostructured $NiFe_2O_4$ with 30 nm particle size shows superparamagnetic doublet that confirms the presence of smaller sized particles in the specimens. Zero field cooled and field cooled curves from 30 nm sized $MnFe_2O_4$ particles showed a peak at T_B (~ 125 K), typical of superparamagnetic blocking temperature. These results are explained in terms of core/shell structure of the materials. The d.c. resistivity of the doped specimens decreases by atleast five orders of magnitude compared to pure sample. This is ascribed to the presence of an interfacial amorphous phase between the sites.

Acknowledgement

The work was supported by a grant from the Nano Science and Technology Initiative of the Department of Science and Technology, New Delhi.

References

Bogomolov V N, Kudinov E K and Firsov Y A 1968 *Sov. Phys. Solid State* **9** 2502

Bramha P, Mitra S and Chakravorty D 1991 *Eur. J. Solid State Inorg. Chem.* **28** 1139

Chatterjee A, Das D, Pradhan S K and Chakravorty D 1993 *J. Magn. Magn. Mater.* **127** 214

Ferele M and Baberschke K 1987 *Phys. Rev. Lett.* **58** 511

Kundu T K and Chakravorty D 1999 *J. Mater. Res.* **14** 3957

Li J E, Dai X, Chow A and Viehland D 1995 *J. Mater. Res.* **10** 926

Mishra S, Karak N, Kundu T K, Das D, Maity N and Chakravorty D 2006 *Mater. Letts* **60** 1111

Mishra S, Kundu T K, Barick K C, Bahadur D and Chakravorty D 2006 *J. Magn. Magn. Mater.* **307** 222

Mott N F 1969 *J. Non-Cryst. Solids* **1** 1

Nathani H, Gubbala S and Misra R D K 2005 *Mater. Sci. & Eng.* **B121** 126

Sato T, Iijima T, Seki M and Inagaki N 1987 *J. Magn. Magn. Mater.* **65** 252

Tang X, Sorensen C M and Klabunde K J 1991 *Phys. Rev. Lett.* **67** 3602

Xu Z, Dai X and Viehland D 1995 *Phys. Rev.* **B51** 6261